Supplementary Information

S1. Experimental

Materials: We used PEG-DA (Mn = 700, Aldrich) and ETPTA (Mn = 428, Aldrich) with 10 wt% of photoinitiator (2-hydroxy-2-methylpropiophenone, 97%, Aldrich) as the photocurable resin. For synthesis of fluorescent silica beads, fluorescein isothiocyanate (FITC, Fluka), Rhodamine B isothiocyanate (RITC, Sigma), aminopropyltriethoxysilane (APS, Aldrich), tetraethyl orthosilicate (TEOS, Aldrich) and NH_4OH (28%, Daejung) are used.[S1]. 3-trimethoxysilyl propyl metacrylate (TMSPMA, Aldirch) is used for the immobilization of 3D structures to the glass. For synthesis of superparamagnetic Fe_3O_4 nanoparticles, $FeCl_3$, (laboratory reagent grade, Fischer Scientific), polyacrylic acid (Mn = 1800, Aldrich), diethylene glycol (99%, Daejung), NH_4OH (28%, Daejung), NaOH (98%, pellet, Daejung) are used[S2].

Synthesis of superparamagnetic Fe_3O_4 nanoparticles: A $FeCl_3$/DEG stock solution is prepared by dissolving 20 mmol $FeCl_3$ in 50 mL of DEG and heating it at 120 °C for 1 h under a nitrogen atmosphere. A NaOH/DEG stock solution is also prepared by dissolving 50 mmol of NaOH in 50 mL of DEG and heating it at 120 °C for 1 h under a nitrogen atmosphere. The superparamagnetic Fe_3O_4 core nanoparticles with tunable size are synthesized by using a high-temperature hydrolysis reaction with PAA as a surfactant. In a typical synthesis, a mixture of 288 mg of PAA, 1 mL of $FeCl_3$ stock solution and 15 mL of DEG is heated to 220 °C in a nitrogen atmosphere for 90 min with vigorous stirring to form a transparent, light yellow solution. Then, 1.8 mL of NaOH/DEG stock solution is injected into the above solution which slowly turned black after about 2 min. The resulting mixture is further heated for 1 h to yield about 120 nm Fe_3O_4 colloids. The synthesized Fe_3O_4 colloids are first washed with a mixture of deionized (DI) water and ethanol, then with pure water several times, and finally dispersed in 3 mL of DI water. The silica coating on Fe_3O_4 nanoparticles is performed using a modified Stöber method. Typically, 3 mL of a Fe_3O_4 colloids solution is mixed with ethyl alcohol (20 mL), NH_4OH (28%, 1 mL). TEOS (0.1 mL) is injected into the solution. After 20 min, TEOS (0.1 mL) is injected one more time. After the reaction finished, the Fe_3O_4/SiO_2 particles are collected by magnetic separation, followed by rinsing with ethanol 3 times and finally dispersed in 3 mL of EtOH.

Optical setup: We used an optofluidic maskless lithography system for the photopolymerization. The microcups are generated by a UV projection pattern generated by a digital micromirror device (DMD, Texas Instruments) using an optofluidic maskless lithography (OFML) system (Figure 1D). In the projection exposure, a ×10 (N.A. = 0.3) or a ×20 objective lenses (N.A. = 0.45) are used to project the image reflected by the DMD onto the prepolymer resin. A high-intensity mercury–xenon lamp (200W bulb) is used for ultraviolet photopatterning combined with a digital micromirror device to dynamically control the shape of polymerized microparticles.

Exposure patterns on the digital micromirror device are controlled by a customized computer program. The UV lamp and DMD was manually equipped with an Olympus IX71 optical microscope. The Olympus IX71 has a wide-excitation blue and green filter set (11012v2, 11007v2, Chroma) for fluorescent microscopy. Visual alignment for photopolymerization was observed with a CCD (charge-coupled device) camera (DP72).

Fabrication of microcarrier arrays: First, 3-trimethoxysilyl propyl metacrylate (TMSPMA) and PDMS are coated and thermally cured on glass substrates at 100 □ for 1 min and at 150 □ for 10 min respectively. Coated PDMS prevents adhesion so that the hydrogels can be easily removed while use of TMSPMA results in hydrogel surface adherence[S3]. The cover slips (150 mm × 150 mm × 0.15 mm) are placed between the glass substrates, where the 3 × 3 microwell array is fabricated with FITC-silica bead-embedded polyethylene glycol diacrylate (PEG-DA). The UV pattern is exposed for 0.1 sec. After generation of the microwell array, the PDMS-coated glass substrate and the spacers are removed and the hydrogels are washed with EtOH and DI water thoroughly. Hydrogels remain bonded to the TMSPMA, which prevents the fabricated hydrogels from coming off the glass substrate during washing.

Cell culture and preparation: HeLa and T24 cells used in experiments were cultured on tissue culture polystyrene in Dulbecco's modified Eagle medium (DMEM with 4.5 g l−1 glucose and 10% FBS, Sigma) and incubated at 37°C in 5% CO_2 and 95% air until near confluence. Cells were detached from culture flasks by trypsinization with 0.25% trypsin and 0.13% EDTA in phosphate-buffered saline. For staining of cells, 1% of propydium iodide (PI, Sigma) was added to cell culture dishes and incubated for 30min.

S2. FE-SEM image of superparamagnetic Fe_3O_4 nanoparticles

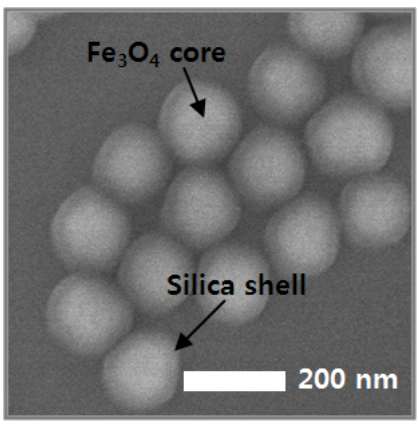

Figure S1. FE-SEM image of the synthesized Fe_3O_4 nanoparticles.

S3. Mass magnetization curve of Fe_3O_4 nanoparticles

The magnetic property of the Fe_3O_4 nanoparticles is characterized using SQUID magnetometer. Figure S2 shows the mass magnetization curve of 150 nm Fe_3O_4 nanoparticles versus the applied magnetic field at 300 K

by cycling the field between -20 to 20 kOe. The sysnthesized Fe_3O_4 nanoparticles are superparamagnetic at room temperature, showing no remanence or coercivity. The saturated mass magnetization of the nanoparticles at 300 K is 37.9 emu·g^{-1}.

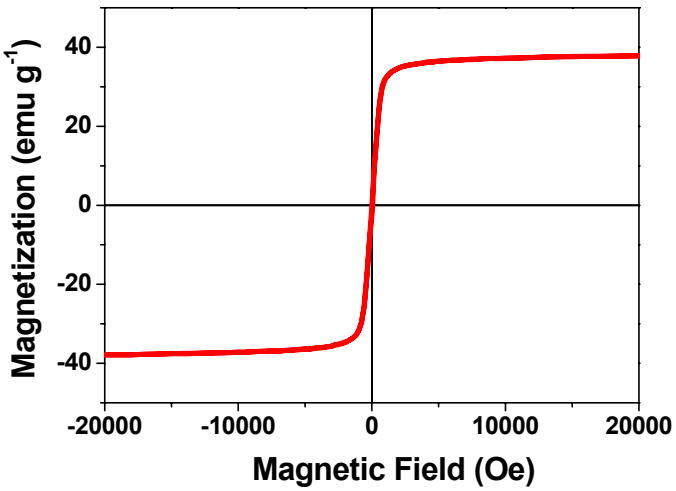

Figure S2. Mass magnetization curve of Fe_3O_4 nanoparticles. The particles have superparamagnetic property at room temperature.

S4. Beam pattern propagation analysis

The formation of a cup-shaped structure from a ring-shaped mask can be explained by applying scalar diffraction theory[S4]. To obtain light intensity distribution near an image plane, we considered a single-lens optical projection system corresponding to our lithography system. Specifically, a mask pattern is considered to be illuminated by UV light, which is assumed to be normally incident, incoherent and polychromatic with a narrow-band wavelength distribution, to form an image intensity distribution in (x, y) plane at various beam propagation distances. The projection lens was assumed to have a square lens aperture with a diagonal length of 8.1mm. All constants or coefficients including numerical aperture and focal length of the lens used in this section are listed in Table S1. Under the assumption of paraxial ray considerations, the light intensity distribution near the image plane can be approximately described as

$$I_i(x,y,z) = \left|h(x,y,z)\right|^2 \otimes I_g(x,y), \qquad z = z_i + \Delta z,$$

$$h(x,y,z) = \frac{1}{\lambda^2 z_0 z}\iint P(\xi,\eta)\exp\left[j\frac{\pi}{\lambda}\left(\frac{1}{z_0}+\frac{1}{z}-\frac{1}{f}\right)\left(\xi^2+\eta^2\right)\right]\exp\left[-j\frac{2\pi}{\lambda z}(x\xi+y\eta)\right]d\xi d\eta,$$

where I_g is the intensity distribution of an ideal image, $\otimes$ is the convolution integral, z is the propagation distance from the projection lens, z_i is the propagation distance for the image plane, Δz is the deviation from the image plane along the z-axis, z_0 is the distance between a mask and the projection lens, λ is a light wavelength, P is a pupil function in (ξ, η) plane, and f is a focal length of the projection lens. In-plane light intensity

distributions depending on the variation of Δz are calculated in consideration of a ring-shaped mask pattern as displayed in Figure 1Ciii, clearly showing various sectional views of a cup-shaped microparticle. Figure 1Ci shows a cross-sectional view of light intensity distribution across *x*-*z* plane with y-axis fixed at the diametral line of the ring-shaped mask pattern. To construct the cross-sectional view we integrated individual *x*-*y* planar light intensity distributions with a *z*-dimensional resolution of 1μm.

In addition to the beam propagation based on diffraction of light, absorption of light energy by molecules is also considered. Since phototoinitiator absorbs light energy through photopolymerization, the light intensity is decreased along *z*-direction as the light propagates inside the medium, following Beer's law

$$\frac{\partial I(z)}{\partial z} = -\varepsilon[PI]I(z)$$

where ε is the molar extinction coefficient of the photoinitiator and [PI] is the concentration of the photoinitiator.[S5]. The effect of absorption was applied to the range of $\Delta z > 0$ by setting the *z*-directional position of the image plane to be located at the surface of substrate. By arbitrary determining the gel point, an estimated particle shape was obtained to reconcile with the experimental result in Figure 1Bi.

Table S1. Parameters used in this work

Parameter	Value [Unit]	Source
UV center wavelength in a vacuum	365 [nm]	-
Refractive index of ETPTA	1.471 [-]	S6
Focal length of the projection lens (*f*)	9 [mm]	S7
Numerical aperture of the projection lens	0.45 [-]	S7
Distance between mask and lens (z_0)	189[mm]	S7
Molar extinction coefficient of the photoiniator (ε)	1.6 [m^3/(mol m)]	S5
Concentration of the photoinitiator ([PI])	1014 [mol/m^3]	-

S5. Movie: Magnetic manipulation of a cell microcarrier

Please add the movie file here.

References

S1. A. Imhof, M. Megens, J. J. Engelberts, D. T. N. de Lang, R. Sprik, W. L. Vos, *J. Phys. Chem. B*, 1999, **103**, 1408-1415.

S2. J. Ge, Y. Yin, *Adv. Mater.*, 2008, **20**, 3485-3491

S3. V. A. Liu, S. N. Bhatia, *Biomed. Microdev.*, 2002, **4**, 257-266.

S4. J. W. Goodman, Introduction to Fourier Optics, **2005**, Robert & Company Publishers

S5. D. Dendukuri, P. Panda, R. Haghgooie, J. M. Kim, T. A. Hatton, P. S. Doyle, *Macromolecules*, 2008, **41**, 8547

S6. Sigma-Aldrich (www.sigmaaldrich.com)

S7. Olympus, Microscope components guide